Hydrol. Earth Syst. Sci. Discuss., 11, 6993–7017, 2014
www.hydrol-earth-syst-sci-discuss.net/11/6993/2014/
doi:10.5194/hessd-11-6993-2014

Hydrology and Earth System Sciences
Open Access
Discussions

An effective parameterization to quantify multiple solute flux breakthrough curves

E. Bloem[1,2], **M. de Gee**[3], **and G. H. de Rooij**[4]

[1]Soil and Environment Division, Bioforsk, Norwegian Institute for Agricultural and Environmental Research, Ås, Norway
[2]Soil Physics, Ecohydrology and Groundwater Management; Environmental Sciences Group, Wageningen University, Wageningen, the Netherlands
[3]Biometris, Wageningen University, Wageningen, the Netherlands
[4]Soil Physics Department, Helmholtz Centre for Environmental Research – UFZ, Halle, Germany

Received: 4 May 2014 – Accepted: 23 May 2014 – Published: 27 June 2014

Correspondence to: E. Bloem (esther.bloem@bioforsk.no)

Published by Copernicus Publications on behalf of the European Geosciences Union.

Abstract

To understand soil and groundwater contamination we study the temporal and spatial aspects of solute transport in the unsaturated zone. One monitoring instrument that captures both aspects is the multi-compartment sampler (MCS). With the MCS developed by Bloem et al. (2010) we are able to measure the downward solute fluxes in 100 compartments at the depth of installation of the MCS, with a minimal disturbance of the flow field. Over time this dataset results in 100 individual solute flux breakthrough curves (BTCs) (temporal aspect). Sorting the BTCs in descending order of solute mass gives the spatial solute distribution curve (spatial aspect).

We present a method to quantitatively characterize datasets gathered with MCS (or single samplers installed at multiple locations in a field at the same depth). The method approximates the full set of breakthrough curves using only a single function with four to eight parameters, which combines both temporal and spatial effects of solute transport in soils. This is achieved by modeling the scaled solute flux density breakthrough curves (BTC_F) for each compartment as the solution of a conventional one-dimensional equilibrium convection disperion equation (CDE), without modifications. We detect and parameterize any relationships between the resulting transport velocities and dispersion coefficients of the individual BTC_Fs. Finally the spatial aspect is parameterized using the Beta distribution.

This method is based on the flux density BTCs directly, which for transport phenomena is preferred over solute concentrations. In three experiments on undisturbed soils, the resulting approximation matched the data well.

1 Introduction

Pollution in soils is a widespread problem and needs to be understood to improve risk assessment, monitoring, and treatment strategies. Both spatial and temporal aspects of solute transport are important to understand soil and groundwater contamination.

HESSD
11, 6993–7017, 2014

Solute transport is strongly influenced by soil heterogeneity which affects both travel time and spatial distribution. One observational method that captures both spatial and temporal aspects of solute transport is the multi-compartment sampler (MCS), either installed underneath a soil column in the laboratory (Quisenberry et al., 1994; Poletika and Jury, 1994; Buchter et al., 1995; Stagnitti et al., 1998; de Rooij and Stagnitti, 2000; Strock et al., 2001) or in situ (Boll et al., 1997; Bloem et al., 2009, 2010).

Solute fluxes are the relevant quantities to estimate solute travel times (e.g. Dagan et al., 1992) and thereby quantify solute transport (Bloem et al., 2008). The multi-compartment sampler (MCS) developed by Bloem et al. (2010) is capable of applying variable suction that corresponds to the ambient pressure head, making it is possible to minimize disturbance of the flow field and measure downwards solute fluxes. The 100 compartments of the instrument are all individually monitored for the amount of water passing through. For each compartment the percolated water can be extracted in situ and analyzed in the laboratory. Extracting and analyzing the captured percolate repeatedly generates 100 individual solute flux breakthrough curves. To organize the large amount of temporal and spatial solute transport data the leaching surface has been developed (de Rooij and Stagnitti, 2002a, b, 2004). This representation combines temporal and spatial aspects of solute leaching. The breakthrough curve (BTC) captures the temporal aspect of solute leaching, which describes the travel time of solutes at a given depth (Jury and Roth, 1990), while the spatial solute distribution curve (SSDC) describes the spatial aspect (Stagnitti et al., 1999; de Rooij and Stagnitti, 2000).

Although the leaching surface provides a tool to visually characterize the spatial and temporal variations of solute movement through the soil, in order to compare datasets (from different experiments and/or from different soils) a quantitative analysis is needed. Although Beven et al. (1993) showed that soils have complex pore geometry and heterogeneous structures which are not fully understood, the various drivers of solute spreading are often lumped in the dispersion coefficient of the convection-dispersion equation (CDE) to provide a relatively straightforward description of solute

HESSD
11, 6993–7017, 2014

transport. Beven et al. (1993) argued that the CDE might be applicable in a functional sense. The mean transport velocity reflects the mass flux of water averaged over some unit area in the system, and the effective dispersion coefficient accounts for the complexities of the flow pathways and heterogeneity in local fluid velocities in the direction of the flow. In this paper we will show that by analyzing a set of BTCs we can use the (considerable) variation of the mean travel times for the individual BTCs as an additional desciptor of the effects of soil heterogeneity on solute transport.

We parameterize solute flux densities directly from BTCs of the solute flux density (BTC_Fs). We developed a method to quantitatively characterize leaching surfaces, which arise by ordering a collection of BTC_Fs according to their accumulated solute content. This is achieved by a separate parameterization of the spatial and temporal aspects of solute leaching. For the temporal aspect, we determine the parameters of the individual BTC_Fs by curve-fitting the velocity and dispersion coefficient of a solution of the convection-dispersion equation. We then detect and parameterize any relationships between the transport velocities and dispersion coefficients of the individual BTC_Fs. The spatial aspect is parameterized using the Beta distribution as outlined by Stagnitti et al. (1999) and de Rooij and Stagnitti (2000, 2004). By combining the temporal and spatial parameterizations we obtain one single function with four to eight parameters that describes the full set of breakthrough curves. The best-fit parameters thus provide a quantitative and objective representation of the leaching surface. This allows a quantitative description of leaching surfaces, providing a means to objectively compare leaching characteristics of different soils, or of the same soil in different seasons. We present the theory and apply this method to three leaching surfaces acquired in a field experiment (metal and membrane sampler experiment) and a laboratory experiment (nylon sampler experiment) in which we used the MCS by Bloem et al. (2010). The same method can be used if instead of a multi-compartment sampler single samplers are used at multiple locations collecting a set of breakthrough curves during a single experiment (same conditions, same soil).

HESSD
11, 6993–7017, 2014

2 Multi-compartment sampler experiments

2.1 Dutch field experiment with metal and membrane samplers

A tracer experiment (Bloem et al., 2009) with two variable-suction multi-compartment samplers (Bloem et al., 2010) was performed in the field. The first MCS had metal porous plates (metal sampler) and the second MCS had a porous membrane (membrane sampler). Each sampler had 10×10 sampling compartments. The compartments of the metal sampler each had a sampling area of 10.35 cm^2. This sampler was installed in the field (Vredepeel, the Netherlands) at 31 cm depth. The membrane sampler had compartments of 10.57 cm^2. This sampler was installed in the same field at 25 cm depth. Both samplers were installed by tunneling from a trench, thus ensuring that the soil above them remained undisturbed. The trench and the tunnel were backfilled to minimize their effect on the flow field. Only the percolate extraction tubes, air suction tube, and wiring for the electrical components were lead above ground. Full details are in Bloem et al. (2009).

On 14 December 2005, a 1 M $CaCl_2 \cdot 2H_2O$ solution tracer was applied on the soil surface above each sampler. To eliminate the side effects of converging and diverging streamlines of the chloride concentration, the tracer solution was applied on 0.70 m × 0.70 m plots. Each application area was covered with a 21 × 21 cell PVC grid, with a syringe holder in the center of each cell. For each plot, we filled 441 medical 10 mL syringes with 5 mL tracer solution (CV = 0.7 %), and placed these in the syringe holders. We then emptied all syringes within two minutes to achieve a spatially uniform tracer pulse.

After each natural rainfall event, usually a cluster of small rain showers (of which 11 occurred during the experiment), the collected leachate was extracted from the sampling compartments while leaving the samplers buried in situ. The collected volumes were determined and the solute concentrations were derived from the EC as measured with an EC meter (Cond 315i and TetraCon325 from WTW; individually calibrated). After 145 days (11 sampling rounds), nearly all tracer had passed the

HESSD
11, 6993–7017, 2014

sampling depth. The mass collected during the final sampling round was less than 0.01 % of the applied mass over the sampling areas. The results of this experiment are described in Bloem et al. (2009).

2.2 Australian laboratory experiment with nylon sampler

For a laboratory experiment we used a variable-suction multi-compartment sampler (Bloem et al., 2010) with a nylon cover (nylon sampler). The nylon sampler consisted of 10 × 10 compartments, each with a sampling area of 10.35 cm^2. A soil monolith of an Australian soil (length 43 cm × width 43 cm × height 29 cm) was placed on top of the nylon sampler. Bloem et al. (2010, 2014) give full details about the set-up and the soil monolith.

With this set-up, a leaching experiment was performed. We uniformly applied a pulse of 8 mm of 3.699 g L^{-1} NaBr solution above the sampler over an area of 35 cm × 35 cm. The pulse was leached out by artificial rain showers of 71 mm each (rainfall rate: 8 mm h^{-1}). During and after each water application event, we collected leachate samples as often as required to prevent individual sample collection compartments from overflowing. The collected volumes were measured and the solute concentration was determined by ion chromatography (US EPA method 300). After 400 mm of drainage, nearly all tracer had passed the sampling depth. The results of this experiment are described in Bloem et al. (2014).

3 Flux density fitting procedure

The outflow area of a multi-compartment sampler is divided into small compartments with the positions of their centers indicated by Cartesian coordinates (x_i, y_j) [L]. The effluent into these compartments is collected at several points t_k [T] in time, and each time the volume V [L^3] of collected drainage and its solute concentration C [M L^{-3}] are measured. Their product gives the collected solute mass. By dividing the mass by the

HESSD
11, 6993–7017, 2014

compartment area and by the sampling time interval $t_k - t_{k-1}$, the solute flux density is found. The results per compartment as a function of time give the solute flux density breakthrough curves BTC_Fs.

The leaching surface is obtained by ranking the sampling compartments in decreasing order of their total collected solute over the entire leaching period, and then plotting the corresponding breakthrough functions BTC_F against the cumulative sampling area s. In this way, the two spatial coordinates x and y are collapsed into a single pseudo-spatial variable s.

de Rooij and Stagnitti (2002a) proposed to scale the solute flux densities by dividing them by the total amount of solute captured to facilitate comparison. The resulting variable $S(s,t)$ has dimensions $[L^{-2}\,T^{-1}]$.

A breakthrough curve (BTC) conveys the temporal aspect of the leaching surface. To characterize the solute flux density BTC (BTC_F) of a single compartment, we used CXTFIT (Toride et al., 1999). The fitted pore water velocity should be interpreted as an average solute velocity, and the fitted dispersion coefficient as a descriptor of the spreading of this solute velocity around its mean. We model the scaled BTC_F (area underneath the curve equal to one) for each compartment as the solution of a conventional one-dimensional equilibrium CDE, without modifications (Toride et al., 1999). In our experiments we used a conservative tracer, and therefore set the retardation factor R to 1 and the degradation and production coefficients to zero. The solute application was modeled as a Dirac delta pulse. We used the solution for flux-averaged concentrations (Toride et al., 1999).

$$C^*(t) = \left(\frac{L^2}{4\pi D t^3}\right)^{\frac{1}{2}} \exp\left(-\frac{(L-vt)^2}{4Dt}\right) \tag{1}$$

with L denoting the depth of the sampling area [L] and C^* the scaled concentration. In our case we use Eq. (1) for the scaled solute flux density instead of the scaled concentration.

HESSD
11, 6993–7017, 2014

The area under each observed BTC_F is represented by parameter C_0. CXTFIT returned the velocity v and dispersion coefficient D as additional parameters to describe the observed BTC_F. With our 100-compartment samplers, that leaves us with 300 parameters. We reduced that number by fitting flexible expressions that related v and D to s:

$$v(s) = a_v s^{b_v} + c_v \quad (2)$$

$$D(s) = a_D s^{b_D} + c_D \quad (3)$$

where a_v, a_D, b_v, b_D, c_v, and c_D are fitting parameters. We now have at most six parameters to describe the temporal redistribution of solutes, but we still have 100 values of C_0 that describe the spatial distribution of the leached solute.

By integrating the leaching surface with respect to t we obtain the spatial solute distribution curve (Stagnitti et al., 1999; de Rooij and Stagnitti, 2000)

$$\mathrm{SSDC}(s) = \int_0^\infty S(s,t)\mathrm{d}t \quad (4)$$

This function represents the spatial aspect of the leaching surface. For each compartment, SSDC(s) is the integral of the corresponding BTC_F. Owing to the ranking of compartments that led to the creation of the coordinate s, SSDC is a non-negative monotonously decreasing function of s. For $S(s,t)$ scaled as indicated above, SSDC integrates to unity over the full range of s, and the value of SSDC and C_0 for any particular s differ only by a constant. Therefore, SSDC(s) can be used equally well as the set of observed C_0 to capture the spatial redistribution of solutes (see de Rooij and Stagnitti, 2000, for a detailed discussion). This is a major advantage over the analysis based on flux concentration BTCs as discussed in Bloem et al. (2012).

The scaled SSDC(s) can often be fitted very well by a Beta distribution (Stagnitti et al., 1999; de Rooij and Stagnitti, 2004)

$$p(x,\alpha,\zeta) = B(\alpha,\zeta)x^{\alpha-1}(1-x)^{\zeta-1}, \qquad 0 \le x \le 1 \quad (5)$$

HESSD
11, 6993–7017, 2014

where p is the probability of the Beta variate as a function of coordinate x,

$$B(\alpha,\zeta) = \frac{\Gamma(\alpha+\zeta)}{\Gamma(\alpha)\Gamma(\zeta)} \tag{6}$$

is the Beta function, and α and ζ are positive shape parameters (de Rooij and Stagnitti, 2004; Nadarajah and Gupta, 2004). The mean, variance and coefficient of variation CV of the Beta distribution are (Gupta and Nadarajah, 2004)

$$\mu(\alpha,\zeta) = \frac{\alpha}{\alpha+\zeta} \tag{7}$$

$$\sigma^2(\alpha,\zeta) = \frac{\alpha\zeta}{(\alpha+\zeta)^2(\alpha+\zeta+1)} \tag{8}$$

$$\mathrm{CV}(\alpha,\zeta) = \sqrt{\frac{\zeta}{\alpha(\alpha+\zeta+1)}} \tag{9}$$

Note that the uniform distribution arises by setting $\alpha = \zeta = 1$, with a coefficient of variation $3^{-1/2}$.

The coordinate x is obtained by scaling s to run from zero to one. We scaled s accordingly, scaled the C_0 values to ensure they added up to one, and then fitted the Beta distribution to describe the scaled C_0 as a function of s. Thus, we found two parameters for capturing the spatial aspect of the leaching surface.

The combination of the six breakthrough-related parameters and the two solute distribution-related parameters yields a quantitative description of the leaching surface. The parametric expression for Eq. (1), using the scaled solute flux densities F^* is given by

$$F^*(s,t) = \left(\frac{L^2}{4\pi\left(a_D s^{b_D}+c_D\right)t^3}\right)^{\frac{1}{2}} \exp\left(-\frac{\left(L-\left(a_v s^{b_v}+c_v\right)t\right)^2}{4\left(a_D s^{b_D}+c_D\right)t}\right) \tag{10}$$

HESSD
11, 6993–7017, 2014

The parametric expression for the leaching surface based on solute flux density (F) combines Eq. (10), the temporal solute breakthrough aspect of solute leaching with Eq. (5), the spatial solute distribution aspect of solute leaching

$$F(s,t) = B(\alpha,\zeta)\left(\frac{s}{s_{\max}}\right)^{\alpha-1}\left(1-\frac{s}{s_{\max}}\right)^{\zeta-1} \cdot \left(\frac{L^2}{4\pi\left(a_D s^{b_D}+c_D\right)t^3}\right)^{\frac{1}{2}} \exp\left(-\frac{\left(L-\left(a_v s^{b_v}+c_v\right)t\right)^2}{4\left(a_D s^{b_D}+c_D\right)t}\right) \quad (11)$$

To reduce irregularities caused by the non-steady input of water, we substituted the time-axis [T] by the cumulative drainage axis [L], measured over the entire sampling area (van Ommen et al., 1989; Jury et al., 1991).

4 Data analysis

We fitted the leaching surfaces of the three experiments (metal sampler, membrane sampler, and nylon sampler) as outlined above. For comparison we also constructed the leaching surface based on flux density directly from the 100 fitted values of v and D, using the observed values of C_0 to scale the fitted BTCs. Hereby we can see how well the CXTFIT program fitted the BTCs. We also constructed the leaching surface by applying the fitted Beta distribution directly to the observed flux density BTCs to see how well the Beta distribution fitted our data.

For the membrane sampler at the Dutch field site, some of the BTCs (those of the compartments that contained little to zero effluent during the experiment) did not converge with CXTFIT, therefore this resulted in a zero velocity. These eight BTCs have not been taken into account when calculating the average velocity and dispersion coefficient. The same holds for a few BTCs of the nylon sampler under the Australian soil monolith in the laboratory.

HESSD
11, 6993–7017, 2014

We calculated the normalized mean root mean square error (RMSE) between the observed and fitted leaching surface by

$$\mathrm{RMSE}_{\mathrm{nm}} = \frac{\sum_{i=1}^{w} \sqrt{\sum_{k=1}^{m} \left(F_{\mathrm{O}}(i,k) - F_{\mathrm{P}}(i,k)\right)^2}}{\sum_{i=1}^{w} \sum_{k=1}^{m} F_{\mathrm{O}}(i,k)} \cdot 100\,\% \tag{12}$$

with subscript O denoting observed solute flux densities, and subscript P indicates their calculated counterparts of the sorted compartments, with w denoting the number of compartments. Counter k indicates the sampling round. The total number of sampling rounds is m.

As the two experiments with the metal and membrane samplers have been performed in the same soil under the same conditions we constructed for those also quantitative leaching surfaces. We sampled the velocity and dispersion values from a normal distribution about the average velocity and average dispersion coefficient creating leaching surfaces which have the same characteristics, thus showing how the same soil might result in visual slightly different leaching surfaces.

5 Results and discussion

In Fig. 1 the leaching surfaces for all three experiments are presented. The leaching surfaces from the two samplers at the Dutch field site with a sandy, fairly moist, hydrophyllic soil are quite similar (Fig. 1a and b), but very different from the leaching surface of the Australian soil (poorly sorted, clayey, with some stones) (Fig. 1c). One individual compartment was dominant in the Australian soil, suggesting the possibility of macropore flow, while at the Dutch soil many compartments were actively receiving solutes although in varying amounts. The Australian soil also required much more drainage to leach the tracer from the soil, indicating the possible presence of areas

HESSD
11, 6993–7017, 2014

of low flow or zones with immobile water (van Genuchten and Wierenga, 1976). For the Dutch soil all compartments were active during the same drainage range. They did not show delayed or second solute outflow peaks.

The SSDCs of the Dutch and the Australian soil again are different (Fig. 2; Table 1) but not as dramatically as the leaching surfaces. The dominant individual compartment received the biggest part of the tracer, but most of the other compartments also received solutes during the experiment. For the two experiments in the Dutch soil, there was no evidence of a single compartment standing out. The tails of all distributions look rather similar. The Beta distribution produced an excellent fit in all cases, even for the Australian soil with one dominating compartment.

The fitted pore water velocities v [$L\,T^{-1}$] and dispersion coefficients D [$L^2\,T^{-1}$] are given in Fig. 3 and Table 1. Pore water velocities appear fairly uniform at the Dutch field site at the scale of the sampling area, but vary between the two samplers. Tracer tests at the end of the experiment revealed no anomalies in the vertical flow above the sampler, and we therefore consider it probable that the difference between the samplers was caused by soil spatial variation at the scale of a few meters. The dispersion coefficients seem to have no convincing trend within either sampler, nor is there a significant difference between the samplers. However, there is a considerable variation within the samplers, resulting in a high CV. In the Australian soil, both the pore water velocity and the dispersion coefficient decrease with increasing s. Here also the variation around the trend for the dispersion coefficient is high. The BTC_Fs of individual cells were fitted well by CXTFIT (small errors in Table 2) and Fig. 4a, b, e, f, i and j shows a good resemblance between fitted and the original scaled BTC_Fs.

5.1 Results related to the Dutch soil experiment in the field

The absence of a trend for the Dutch soil experiments allowed us to replace $v(s)$ and $D(s)$ of the metal and membrane samplers by their respective mean values for all s. The lack of a trend is consistent with efficient lateral mixing, which is considered to be reflecting a convective-dispersive transport mechanism (Flühler et al., 1996). Replacing

HESSD
11, 6993–7017, 2014

the actual measurements by smooth breakthrough curves calculated from fitted v and D increased the normalized mean RMSE for the scaled BTC_Fs significantly (Table 2). The averaged results (Fig. 4c and g) produce less peaky leaching surfaces than those observed at the Dutch field site (Fig. 4a and e); this peaky feature is well preserved when the CXTFIT approximations for each compartment are used, as can be seen in Fig. 4b and f.

In the qualitative approach, we sampled velocity and dispersion values from a normal distribution about the averaged velocity and averaged dispersion coefficient. When we use these parameter values to construct a leaching surface that looks similar to the observed leaching surface, we see that the results for the scaled flux densities show a good resemblance for the metal sampler in the Dutch soil (Fig. 4d). For the membrane experiment, however, the large standard deviation of D and, to a lesser extent, v, generated some excessively large values in the reproduced leaching surface (Fig. 4h).

Replacing the actual measurements by smooth breakthrough curves calculated from fitted v and D and scaled by the value of the fit to the SSDC for the value of s corresponding to each BTC gave somewhat smoother but still accurate leaching surfaces of the flux densities (Fig. 5b, f, and j). We completed the parametric fit of the leaching surfaces by replacing the individual values of v and D by their mean values for the samplers in the Dutch field site (Fig. 4c and g). Applying the Beta distribution to the averaged results does not alter the data any further (Fig. 5c and g). The normalized mean RMSE even improved slightly to 19 % for the metal sampler and 30 % for the membrane sampler (Table 2).

The qualitative results (Fig. 5d and h) better resemble the observed leaching surfaces (Fig. 5a and e), although the highest peak is still much larger for the simulated leaching surfaces than in reality. The characteristics of the observed, parameterized, and qualitative leaching surfaces are all the same though.

The Beta distributions fit the data very well (Fig. 2a and b). Applying the Beta distribution directly to the observed scaled flux densities resulted in Fig. 6b and f. The

HESSD
11, 6993–7017, 2014

normalized mean RMSE related to this fit is 7 % for the metal sampler and 8 % for the membrane sampler.

5.2 Results related to the Australian soil experiment in the laboratory

The Australian soil monolith used in the laboratory exhibited clear trends of v and D with s (Fig. 3); we replaced the individual values $v(s)$ and $D(s)$ by their linear regression fit to produce Fig. 4k.

By applying the Beta distribution to the scaled flux densities for the nylon experiment we obtained the scaled parametric leaching surface based on flux density (Fig. 5k). The smooth fitted leaching surface missed the peak and the narrow BTC of the first dominant compartment, emphasizing the deviation of that compartment from the average behavior as reflected by the fitted surface, which generally represents the observed leaching surface rather well. The normalized mean RMSE here is of the same order as that of the metal sampler (Table 2).

Applying the Beta function directly to the observed scaled flux densities leads to an error of 4 %. The resulting leaching surface (Fig. 6f) does show the first peak of the BTC very well. Also the pattern is identical to the observed leaching surface.

Despite the fact that this fit required five parameters and the fits for both Dutch field-based leaching surfaces only four, the goodness-of-fits (RMSE) were not significantly different (Table 2), reflecting the different natures of the observed leaching surfaces. All fitted leaching surfaces appeared to capture the main pattern of the observed leaching surfaces rather well.

6 Conclusions

By parameterizing the leaching surface we made it possible to quantitatively analyze the leaching behavior of soils. We developed a method to approximate the leaching surface S using only four to eight parameters, which combine both temporal as well

HESSD
11, 6993–7017, 2014

as spatial effects of solute transport in soils. This method is based on the flux density BTCs, which for transport phenomena is preferred over solute concentrations. The resulting approximation showed to have a good resemblance to the leaching surfaces constructed from the observed breakthrough curves.

The method has been successfully used to characterize datasets gathered with multi-compartment samplers. The same method could be used if instead of a multi-compartment sampler single samplers are used at multiple locations collecting a set of breakthrough curves during a single experiment in one field, under the same conditions.

Acknowledgements. This research is supported by the Norwegian Research Council and by the Research Council for Earth and Life Sciences (ALW) with financial aid from the Netherlands Organization for Scientific Research (NWO).

References

Beven, K. J., Henderson, D. E., and Reeves, A. D.: Dispersion parameters for undisturbed partially saturated soil, J. Hydrol., 143, 19–43, 1993. 6995, 6996

Bloem, E., Vanderborght, J., and de Rooij, G. H.: Leaching surfaces to characterize transport in a heterogeneous aquifer: comparison between flux concentrations, resident concentrations, and flux concentrations estimated from temporal moment analysis, Water Resour. Res., 44, W10412, doi:10.1029/2007WR006425, 2008. 6995

Bloem, E., Hogervorst, F., and de Rooij, G.: A field experiment with variable-suction multi-compartment samplers to measure the spatio-temporal distribution of solute leaching in an agricultural soil, J. Contam. Hydrol., 105, 131–145, doi:10.1016/j.jconhyd.2008.11.010, 2009. 6995, 6997, 6998

Bloem, E., Hogervorst, F., de Rooij, G., and Stagnitti, F.: Variable-suction multicompartment samplers to measure spatiotemporal unsaturated water and solute fluxes, Vadose Zone J., 9, 148–159, doi:10.2136/vzj2008.0111, 2010. 6994, 6995, 6996, 6997, 6998

Bloem, E., de Gee, M., and de Rooij, G.: Parameterizing the leaching surface by combining curve-fitting for solute breakthrough and for spatial solute distribution, Transport Porous Med., 92, 667–685, doi:10.1007/s11242-011-9927-2, 2012. 7000

HESSD

11, 6993–7017, 2014

Bloem, E., Hermon, K., de Rooij, G., and Stagnitti, F.: Spatial and temporal distribution of the leaching of surface applied tracers from an irrigated monolith of a loamy vineyard soil, Environ. Sci. Pollut. R., 1–11, doi:10.1007/s11356-014-2637-x, online first, 2014. 6998

Boll, J., Selker, J. S., Shalit, G., and Steenhuis, T. S.: Frequency distribution of water and solute transport properties derived from pan sampler data, Water Resour. Res., 33, 2655–2664, 1997. 6995

Buchter, B., Hinz, C., Flury, M., and Flühler, H.: Heterogeneous flow and solute transport in an unsaturated stony soil monolith, Soil Sci. Soc. Am. J., 59, 14–21, 1995. 6995

Dagan, G., Cvetkovic, V., and Shapiro, A.: A solute flux approach to transport in heterogeneous formations. 1. The general framework, Water Resour. Res., 28, 1369–1376, 1992. 6995

de Rooij, G. H. and Stagnitti, F.: Spatial variability of solute leaching: experimental validation of a quantitative parameterization, Soil Sci. Soc. Am. J., 64, 499–504, 2000. 6995, 6996, 7000

de Rooij, G. H. and Stagnitti, F.: Spatial and temporal distribution of solute leaching in heterogeneous soils: analysis and application to multisampler lysimeter data, J. Contam. Hydrol., 54, 329–346, 2002a. 6995, 6999

de Rooij, G. H. and Stagnitti, F.: The solute leaching surface as a tool to assess the performance of multidimensional unsaturated solute transport models., in: Pre-Conference Proceedings of the International Conference on Computational Methods in Water Resources, Delft, the Netherlands, 23–28 June 2002, doi:10.1016/S0167-5648(02)80119-8, edited by: Hassanizadeh, S. M., Schotting, R. J., Gray, W. G., and Pinder, G. F., 639–646, Elsevier, Amsterdam, the Netherlands, 2002b. 6995

de Rooij, G. H. and Stagnitti, F.: Applications of the Beta distribution in soil science, in: Handbook of Beta Distribution and its Applications, edited by: Gupta, A. K. and Nadarajah, S., Marcel Dekker Inc., New York, 535–550, 2004. 6995, 6996, 7000, 7001

Flühler, H., Durner, W., and Flury, M.: Lateral solute mixing processes – a key for understanding field-scale transport of water and solutes, Geoderma, 70, 165–183, 1996. 7004

Gupta, A. K. and Nadarajah, S.: Mathematical properties of the beta distribution, in: Handbook of Beta Distribution and its Applications, edited by: Gupta, A. K. and Nadarajah, S., Marcel Dekker Inc., New York, 33–53, 2004. 7001

Jury, W. A. and Roth, K.: Transfer Functions and Solute Movement Through Soil, Birkhauser Verlag, Basel, 226 pp., 1990. 6995

Jury, W. A., Gardner, W. R., and Gardner, W. H.: Soil Physics, 5th Edn., John Wiley and Sons Inc., New York, USA, 1991. 7002

HESSD
11, 6993–7017, 2014

Nadarajah, S. and Gupta, A. K.: Beta funtion and the incomplete beta function, in: Handbook of Beta Distribution and its Applications, edited by: Gupta, A. K. and Nadarajah, S., Marcel Dekker, Inc., New York, 1–31, 2004. 7001

Poletika, N. N. and Jury, W. A.: Effects of soil surface management on water flow distribution and solute dispersion, Soil Sci. Soc. Am. J., 58, 999–1006, 1994. 6995

Quisenberry, V. L., Phillips, R. E., and Zeleznik, J. M.: Spatial distribution of water and chloride macropore flow in a well-structured soil, Soil Sci. Soc. Am. J., 58, 1294–1300, 1994. 6995

Stagnitti, F., Sherwood, J., Allinson, G., Evans, L., Allinson, M., Li, L., and Phillips, I.: An investigation of localised soil heterogeneities on solute transport using a multisegment percolation system, New Zeal. J. Agr. Res., 41, 603–612, 1998. 6995

Stagnitti, F., Li, L., Allinson, G., Phillips, I., Lockington, D., Zeiliguer, A., Allinson, M., Lloyd-Smith, J., and Xie, M.: A mathematical model for estimating the extent of solute- and water-flux heterogeneity in multiple sample percolation experiments, J. Hydrol., 215, 59–69, 1999. 6995, 6996, 7000

Strock, J. S., Cassel, D. K., and Gumpertz, M. L.: Spatial variability of water and bromide transport through variably saturated soil blocks, Soil Sci. Soc. Am. J., 65, 1607–1617, 2001. 6995

Toride, N., Leij, F. J., and van Genuchten, M. T.: The CXTFIT Code for Estimating Transport Parameters from Laboratory or Field Tracer Experiments, Version 2.1, Tech. Rep. Research Report No. 137, US Salinity Laboratory, Agricultual Research Service, US Department of Agriculture, Riverside, California, United States, 1999. 6999

van Genuchten, M. T. and Wierenga, P. J.: Mass transfer studies in sorbing porous media. I. Analytical solutions, Soil Sci. Soc. Am. J., 40, 473–480, 1976. 7004

van Ommen, H. C., van Genuchten, M. T., van der Molen, W. H., Dijksma, R., and Hulshof, J.: Experimental and theoretical analysis of solute transport from a diffuse source of pollution, J. Hydrol., 105, 225–251, 1989. 7002

HESSD
11, 6993–7017, 2014

Table 1. Statistics of the population of fitted parameters (v and D for the metal and membrane samplers), the fitted parameter values if only a single fit was required (α and ζ), and the fitted relationship between v and s, and between D and s (nylon sampler).

Sampler		v (cm mm^{-1})	D (cm^2 mm^{-1})	α	ζ
Metal	Mean	0.559	0.516	0.824	3.374
	STDEV	0.099	0.223		
	CV (%)	17.67	43.26		
Membrane	Mean	0.484	0.470	0.800	2.916
	STDEV	0.134	0.402		
	CV (%)	27.81	85.37		
Nylon	Mean	$-2.8663s + 0.3211$	$-7.0388s + 1.0234$	0.689	2.214

HESSD
11, 6993–7017, 2014

Table 2. The normalized mean root mean square error (RMSE) (%) between the observed and parameterized leaching surfaces based on flux density scaled per BTC and between the observed and parameterized scaled leaching surface based on flux density. For the leaching surfaces scaled by each BTC_F the errors have been calculated for the fitted v and D, and for the averaged v and D. For the scaled leaching surface based on flux density we calculated the error for the fit if the Beta distribution has been applied directly on the observed BTC_F, and after the fitted v and D, and after the averaged v and D.

	Fit	normalized mean RMSE (%)		
		Metal	Membrane	Nylon
scaled per BTC BTC_F	Direct	0	0	0
	v and D fitted	10.0	16.3	10.9
	v and D averaged	26.6	40.1	23.4
scaled BTC_F	Direct	6.8	7.9	3.8
	v and D fitted	10.3	14.1	12.1
	v and D averaged	19.6	30.3	20.1

HESSD
11, 6993–7017, 2014

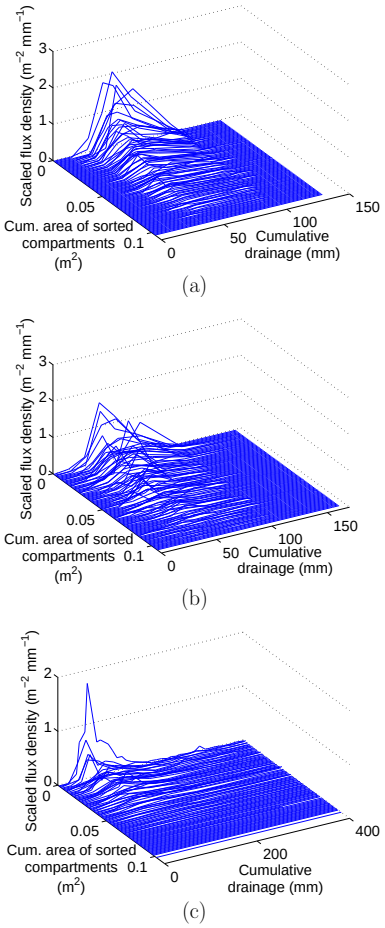

Figure 1. Leaching surfaces based on flux density for the metal sampler experiment **(a)**, the membrane sampler experiment **(b)**, and the nylon sampler experiment **(c)**.

HESSD
11, 6993–7017, 2014

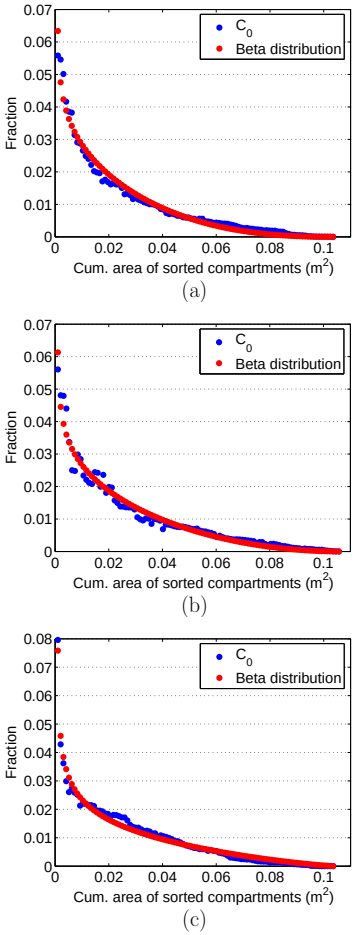

Figure 2. C_0, thus the SSDC for the metal sampler experiment **(a)**, the membrane sampler experiment **(b)**, and the nylon sampler experiment **(c)**.

HESSD
11, 6993–7017, 2014

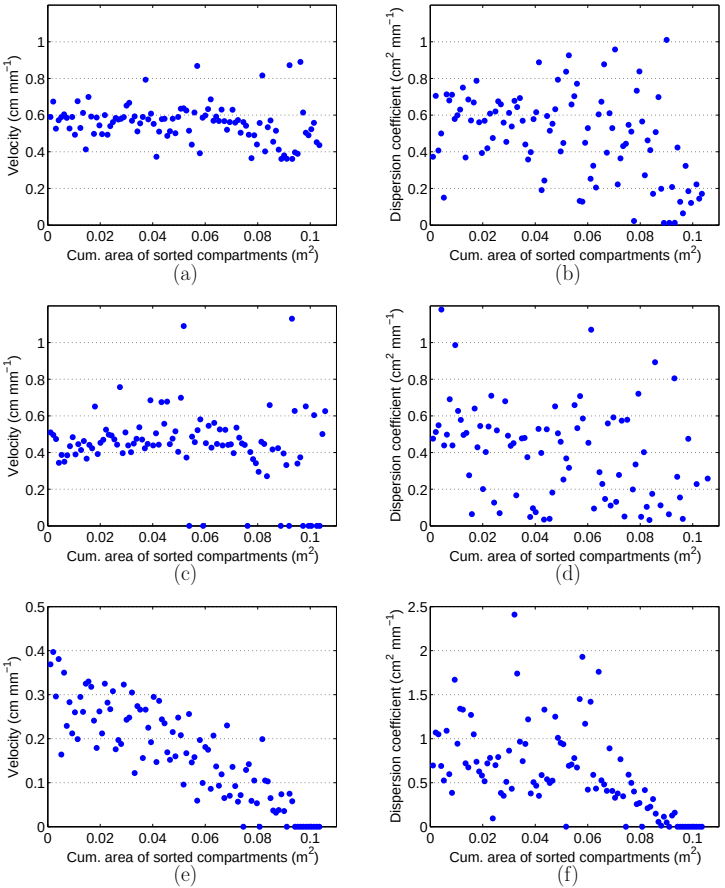

Figure 3. CXTFIT curve fitting results for the velocity v **(a, c, e)** and dispersion coefficient D **(b, d, f)** of the 100 sorted scaled BTC_Fs based on flux density. Results for the metal sampler experiment (**a** and **b**), the membrane sampler experiment (**c** and **d**), and the nylon sampler experiment (**e** and **f**).

HESSD
11, 6993–7017, 2014

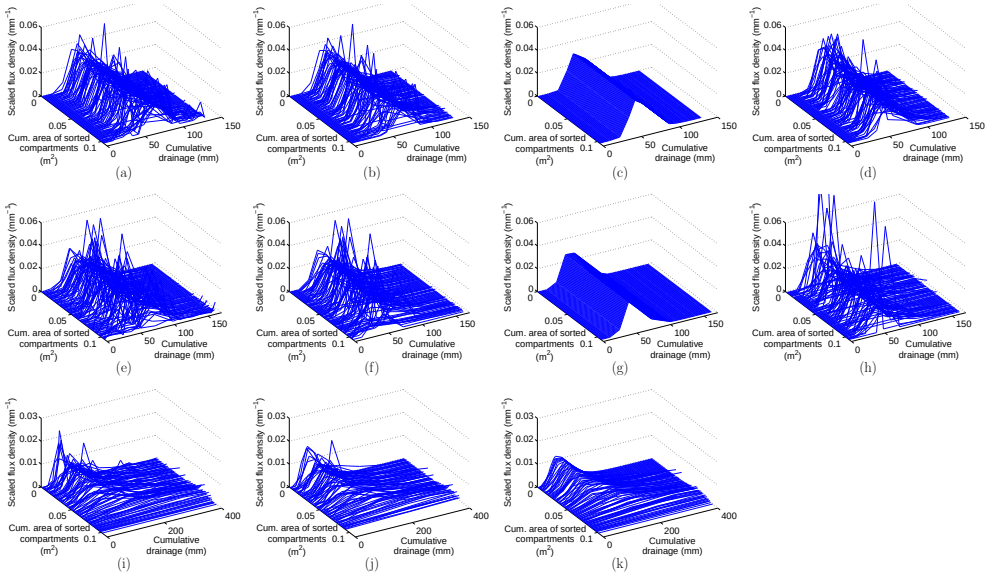

Figure 4. The observed scaled leaching surface based on flux density **(a, e, i)**, with all individual breakthrough curves scaled to integrate to unity. The scaled leaching surface based on flux density for the calculated v and D per BTC_F, fitted with CXTFIT **(b, f, j)**, the scaled leaching surface based on flux density with the average v and average D as given in Table 1 **(c, g, k)**, and the scaled leaching surface based on flux density with a qualitative approach **(d, h)**. Results for the metal sampler experiment **(a–d)**, the membrane sampler experiment **(e–h)**, and the nylon sampler experiment **(i–k)**.

HESSD
11, 6993–7017, 2014

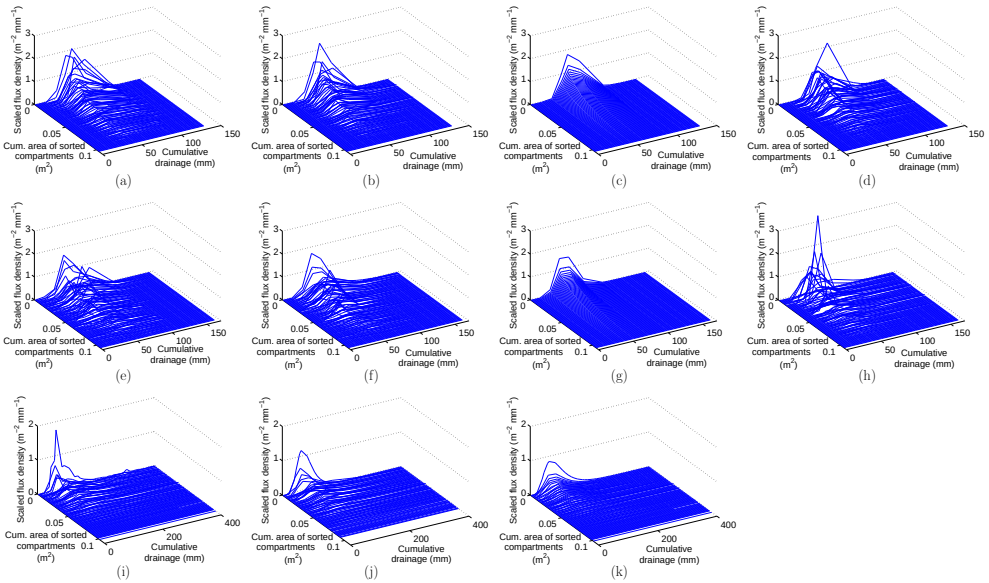

Figure 5. The observed scaled leaching surface based on flux density **(a, e, i)** and parameterizations: scaled leaching surfaces based on flux density are constructed on the calculated v and D per BTC_F together with the fitted Beta distribution **(b, f, j)**, the average v and D (Table 1) with the fitted Beta distribution **(c, g, k)**, and a qualitative fit of v and D together with the fitted Beta distribution **(d, h)**. Results for the metal sampler experiment **(a–d)**, the membrane sampler experiment **(e–h)**, and the nylon sampler experiment **(i–k)**.

HESSD
11, 6993–7017, 2014

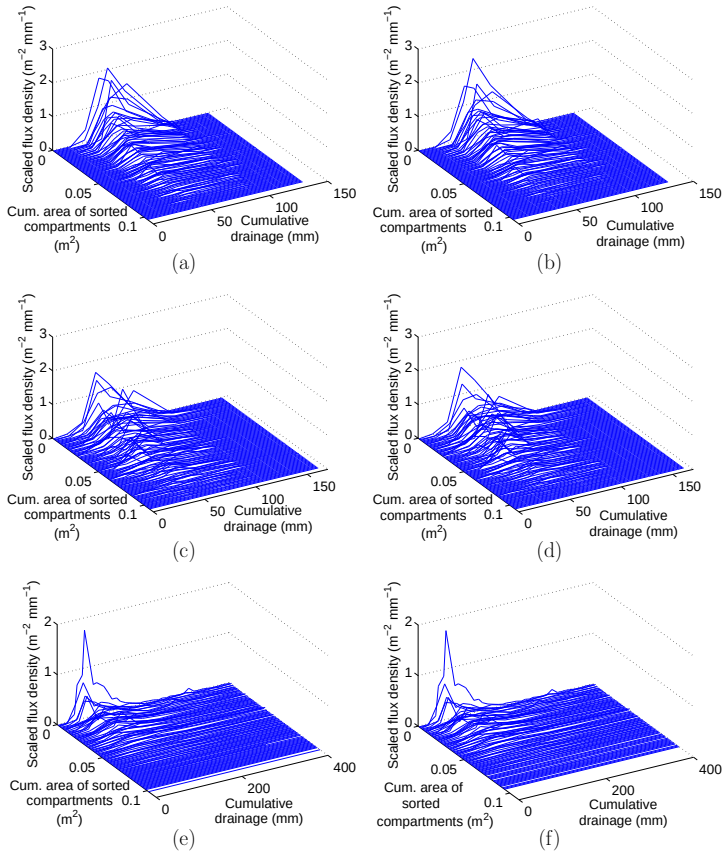

Figure 6. The observed scaled leaching surface based on flux density **(a, c, e)** and parameterization: scaled leaching surface based on flux density constructed on the observed scaled BTC_F together with the fitted Beta distribution **(b, d, f)**. Results for the metal sampler experiment **(a, b)**, the membrane sampler experiment **(c, d)**, and the nylon sampler experiment **(e, f)**.

HESSD
11, 6993–7017, 2014